Recent Results from the USU Plasma Impedance Probe for the NASA E-Winds Sounding Rocket Campaign

Chad G. Carlson
Advisor: Dr. Charles M. Swenson

Abstract— **The new plasma impedance probe built by Utah State University was flown on July 1, 2003 as part of a NASA sounding rocket campaign to investigate midlatitude plasma layers and neutral winds. The instrument provided measurements of absolute and relative electron densities for the mission. The instrumentation technique is briefly introduced, along with the plasma parameters that the technique is capable of measuring. Relative electron densities from the DC Langmuir probe for the mission are presented along with a comparison of the relative density data to the absolute density provided by the plasma frequency probe.**

I. Introduction

As a magnetized, ionized medium surrounding the Earth, the ionosphere directly affects a number of critical space and earth systems. It is the chief barrier in radio frequency communication with spacecraft. Since it has an abundance of charged particles, the ionosphere is responsible for spacecraft charging, which has led to failures of some satellites or their various subsystems[1]. Ionospheric irregularities can create severe scintillations in Global Positioning System (GPS) signals leading to significant errors in critical navigational and guidance systems [2][3]. Additionally, large geomagnetic currents in the ionosphere have caused power distribution systems to fail, such as the failure that occurred in Canada in 1989 [4]. Due to the effects that the ionosphere can have on critical space and earth systems, it is important that engineers and scientists understand the underlying physics that drive the phenomena. Such an understanding aids the design of robust systems that are immune to these space weather effects.

Electron density is often considered the primary parameter of a plasma. Instrumentation techniques have been developed since the early 1920's to make *in-situ* electron density measurements in a plasma, beginning with the pioneering work of Langmuir and Mott-Smith. Langmuir probes measure the plasma environment via a current collected on a conducting surface that has been charged with an applied potential and have been studied extensively[5]. Impedance probes allow plasma parameters to be observed via changes in the impedance of an antenna immersed in the plasma environment. These effects were first observed experimentally by Jackson in 1961[6]. As a radio frequency (RF) signal is swept in frequency, impedance probes measure the variations in the antenna input impedance. At fundamental plasma frequencies, the plasma particles oscillate resulting in drastic changes in the antenna's frequency response.

The plasma frequency probe (PFP) is an impedance instrument that has been built at Utah State University (USU) since the 1960's [7]. The PFP has been an integral part of many sounding rocket payloads. Recent campaigns that have flown the instrument include CODA I (21.121), CODA II (21.128), SAL (21.117), Thunderstorm II (38.007), Thunderstorm III (36.111) and Auroral Turbulence (40.005)[8].

The latest generation instrument from USU is known as the plasma impedance probe (PIP). The PIP is an integrated suite of instruments, including a PFP, for observing absolute and relative electron densities, magnetic field strength, and electron-neutral collision frequency. On July 1, 2003, the PIP flew as an integral component of four sounding rocket payloads (41.036, 41.037, 27.144, and 41.038) as part of NASA E-Winds campaign from Wallops Island, Virginia. This paper details the functionality of the PIP built for the E-Winds sounding rocket campaign and the preliminary results from that mission. Antenna impedance in a plasma will be briefly introduced. The construction and operation of the PIP instrument will then be presented. The E-Winds sounding rocket campaign will be briefly discussed followed by an analysis of the data obtained from each of the PIP instruments for the E-Winds mission.

II. Antenna Impedance in a Plasma

A plasma can be represented as a dielectric with a relative permittivity, ϵ_r, that is a function of its density, temperature, collision frequency, and magnetic field. When an antenna is immersed

C. Carlson is a graduate student at Utah State University. E-mail: chad.carlson@usu.edu

in a plasma, the dielectric properties of the the plasma modify the input impedance of the antenna. The impedance modifications are directly related to fundamental plasma parameters, and hence the measurement of an antenna's impedance in a plasma provides a method of measuring the space environment.

In 1963, Balmain constructed a closed-form analytical solution for the impedance of a short dipole in a magnetoplasma[9]. Limiting his analysis to electrically short antennas, Balmain assumed a linear current distribution and used a quasi-static electromagnetic theory to compute the antenna's input impedance. For a 100 cm long, 1 cm radius dipole antenna whose orientation angle with the magnetic field denoted by θ is varied from $0-90^o$, a simple simulation gives the impedance curves predicted by Balmain's theory for a plasma frequency, f_p, of 1 MHz, a cyclotron frequency of $0.7f_p$, and an electron-neutral collision frequency of $0.02f_p$.

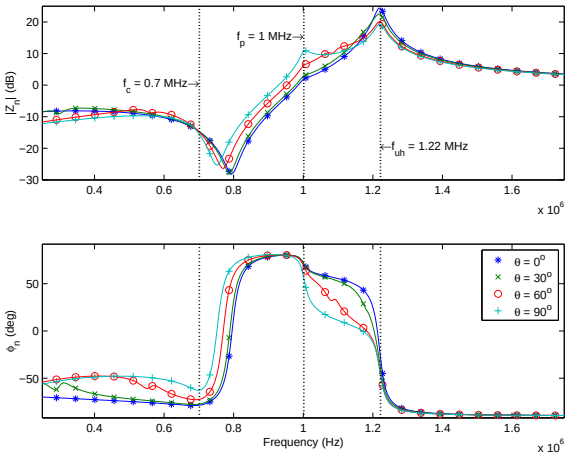

Fig. 1. Balmain theory for a small rocket antenna in the E-region of the ionosphere

Fig. 1 clearly demonstrates two significant resonances due to the plasma's interaction with the antenna: the minimum in the magnitude response corresponding to the phase change from capacitive (-90^o) to inductive ($+90^o$) is called the sheath-plasma "series" resonance, while the maximum in the magnitude response that corresponds to the phase change from inductive to capacitive is the called the "parallel" resonance.

The parallel resonant frequency is nearly equal to the upper hybrid frequency. The slight difference between the parallel resonance and the actual upper hybrid resonance is due to the proximity of the plasma frequency to the upper hybrid frequency. f_p interferes with f_{uh}, producing a slight error in the parallel resonance. In the plots shown in Fig. 1, the amount of error induced by f_p is equal to 2.211 kHz, a 0.18% error. Because the error is much less than 1%, the parallel resonance is often referred to as the upper hybrid resonance.

Since the upper hybrid resonance is so prominent in an antenna's impedance in a plasma, it is easily identified and measured. As a result, the upper hybrid resonance provides the mechanism whereby electron density measurements can be made via an antenna's input impedance, because

$$N_e = \frac{4\pi^2 \epsilon_0 m_e}{e^2} \left(f_{uh}^2 - f_c^2 \right), \qquad (1)$$

where f_c is easily computed from the geomagnetic field strength B.

III. The Plasma Impedance Probe

Physically, the PIP instrument suite consists of an electronics enclosure measuring 5" by 5" by 5", and two boom assemblies that are 1" in diameter and 3' in length. The electronics enclosure provides slots for five printed circuit board (PCB) modules: a telemetry PCB, a science PCB, two input/output (I/O) PCB's and a power PCB. The boom assembly is composed of an antenna, a guarding section, a DC Langmuir probe sensor, and a pre-amplifier section known as the RF head. Both the electronics enclosure and boom assemblies are manufactured with T-6061 aluminum. Physically, the PIP's rugged, modular design and small form factor is ideal for sounding rocket campaigns and could be further refined for small satellite applications.

A. Functions of the PIP

Functionally, the PIP is composed of five instruments: a plasma frequency probe (PFP), a swept impedance probe (PSP), a plasma Q probe (PQP), an experimental ion impedance probe (IRP), and a DC Langmuir probe (DCP). The PFP is a phase-locked loop that tracks the zero phase angle which corresponds to the upper hybrid resonance (f_{uh}). The upper hybrid frequency is closely related to the plasma frequency (f_p), which is directly related to electron density (n_e). The PSP sweeps through a predetermined set of 128 frequencies from 100 kHz to 15 MHz, making magnitude and phase measurements at each frequency. Over the band of frequencies, natural resonances in the plasma are easily identified by corresponding maxima and minima in the magnitude response. The PQP measures the Q or bandwidth of the upper hybrid resonance. The DCP is a fixed-bias Langmuir probe (LP) designed to make high resolution temporal and spatial measurement of relative electron density. Finally, the IRP is an experimental impedance instrument intended to explore ion resonance characteristics at frequencies from 1 kHz to 100 kHz. The measurement capabilities of the five PIP instruments is summarized in table I.

TABLE I
E-Winds PIP Instrument Function Table

PIP Instrument	Sample Rate	Temporal Resolution	Spatial Resolution	Frequency Resolution	Plasma Measurement
PFP	3.58 kHz	0.279 ms	0.05 - 0.39 m	500 Hz	n_e, f_{uh}
PSP	3.58 kHz	35.75 ms	7.21 - 50.44 m	40-50 kHz	n_e, f_{uh}, T_e?
PQP	1.79 kHz	2.79 ms	0.11 - 0.78 m	NA	Q_{uh}, ν
DCP	3.58 kHz	0.279 ms	0.05 - 0.39 m	NA	n_e
IRP	447 Hz	286.35 ms	57.72 - 404.03 m	767 Hz	f_{lh}?, n_i?

The excellent temporal, spatial, and frequency resolution of the PIP instruments allows us to resolve fine small-scale plasma irregularities. Scientists are often satisfied with resolutions that are an order of magnitude higher than the measurements provided by the PIP. It should also be noted that each of the 5 instruments is built to measure different components of the plasma environment. There is some overlap in the plasma components by the various instruments, which provides redundancy in case of failures. Combining the high resolution, redundant data from each instrument should allow a scientist to construct a powerful empirical model of the plasma environment.

Functionally, the science portion of the PIP may be partitioned into two main components, the RF head PCB and the science PCB. The RF head serves as the impedance transducer of the PIP, while the science board provides the control and data handling for the instrument.

B. RF Head

A block diagram of the RF head is shown in Fig.2. The three principal components of the RF head are the transimpedance measurement and reference amplifiers, the magnitude detector, and the phase detector.

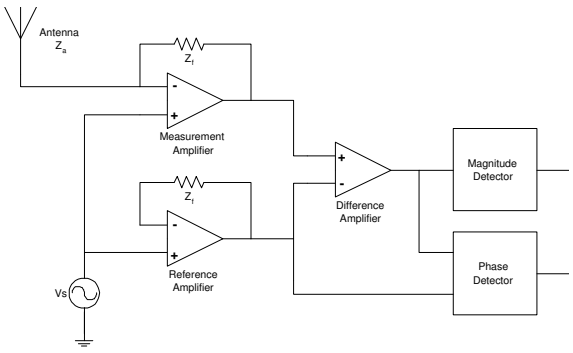

Fig. 2. Block Diagram of RF Head

The RF head measures the impedance of the antenna in plasma, using measurement and reference operational amplifiers followed by a difference amplifier. A low-level RF signal is applied to the non-inverting terminals of the measurement and reference op-amps shown in Fig. 2. Under ideal op-amp assumptions, there is no potential difference across the input terminals, so the signal applied at the non-inverting terminals appears at the inverting terminals simultaneously. Due to the virtual ground across the terminals of the measurement amplifier, the RF input signal at the non-inverting terminal is concurrently applied to the antenna.

In the near field of the antenna, the RF signal exchanges energy with the plasma causing the electrons to oscillate. The oscillating electrons induce additional currents on the antenna that modify its complex input impedance, Z_a. Since an ideal op amp has an infinite input impedance the additional currents are sampled across the feedback impedance, Z_f, producing a voltage at the output of the measurement amplifier.

From basic circuit theory, the output voltage for this non-inverting op amp configuration, which we will call V_1 is given by:

$$V_1 = \left(1 + \frac{Z_f}{Z_a}\right) V_s$$

So the transfer function of the circuit is the gain G given by:

$$G = 1 + \frac{Z_f}{Z_a}$$

As Z_a is modified by the electron oscillations, the gain of the measurement transimpedance amplifier is altered, resulting in voltage variations at the output of the measurement amplifier. Since the feedback network, Z_f, is fixed, an increase in Z_a reduces the gain and vice versa. The reference amplifier has a gain of 1 and buffers the RF input signal, giving an output voltage, $V_2 = V_s$. The reference output is subtracted from the antenna measurement using a difference amplifier. The resulting output is given by

$$\begin{aligned} V_o &= V_1 - V_2 \\ &= V_s \left(1 + \frac{Z_f}{Z_a}\right) - V_s \\ &= \frac{Z_f}{Z_a} V_s, \end{aligned} \tag{2}$$

where V_o is the voltage difference due to the plasma, and is a function of the antenna impedance and Z_f.

The instrument response at the sheath-plasma and upper hybrid resonances can be computed using (2). From Fig. 1 in the previous section we may recall that at the sheath-plasma resonance the magnitude of the antenna's impedance is minimized, which leads to an increase in V_o. At the upper hybrid resonance the antenna impedance magnitude reaches a maximum, resulting in a decrease in V_o. Due to the reciprocal relationship between the magnitude of the antenna impedance and the output of the differential amplifier, we may conclude that the topology of the RF head allows for admittance measurements of the antenna in plasma. Since admittance is the reciprocal of impedance, the impedance is easily determined.

Following the difference amplifier, the measured admittance value of the antenna in plasma is passed to the magnitude and phase detectors. The magnitude detector is a logarithmic amplifier (log amp) that detects the admittance of V_o by demodulating the signal. The digital phase detector is composed of a comparator, two D flip-flops, and a lowpass Bessel filter. The antenna (V_o) and reference (V_2) signals from the transimpedance op-amps are sent to the comparator, which produces square waves corresponding to the sinusoidal inputs. The outputs from the comparator are then sent to a D flip-flop circuit for phase detection. The phase difference between the antenna and reference signals corresponds to a time shift between the input square waves. The time shift between the signals is encoded by the flip-flops into a varying duty cycle square wave output that is integrated by the lowpass filter to give a DC mean that is proportional to the amount of phase shift between the two signals.

C. Science Board

As the admittance and phase measurements are made by the RF head, the science board processes the data and prepares it for the telemetry system. The science PCB may be partitioned into a instrument control and telemetry interface subsystem and a frequency control subsystem. The data from the RF head is first sampled by a 14-bit analog to digital converter on the science board. With an input range of +5 Volts, each count of the A/D converter represents 0.305 millivolts, giving the effective quantization error for the instrument. This implies that with a Z_f of 475 Ω, the instrument can ideally measure plasma induced currents as small as 0.642 μA. The sampled data is then passed to a programmable logic device (PLD) to be processed. The PLD is the central processing unit of the PIP. The PLD uses a combination of finite state machines and registers to control the instrument's operation.

The PLD used in the current iteration of the PIP is an Altera ACEX chip. The ACEX family uses SRAM memory. The SRAM architecture provides a large number of logic gates for design. An external EEPROM configuration chip loads the programming of the PLD into the SRAM memory upon power up. The most attractive feature of the Altera device is that it is in-system reprogrammable, that is to say the digital program for the PLD can be changed without removing the component from the board. Using a computer and interface cable, the device may be reprogrammed with a different digital design up to 50,000 times before device failure. In-system reprogrammability affords the ability to constantly update the digital design through testing, calibration, and integration. This allows the cognizant engineer to change control gains that may be needed to tweak the system for optimal performance. The PLD programs the direct digital synthesizer (DDS) to give the needed output frequencies for the various PIP measurements. The DDS is another critical component of the science board. The AD9851 180 MHz direct digital synthesizer was used for the current PIP design. The AD9851 is programmed via a 40-bit digital tuning word, which is clocked into the device in 8-bit words. Of the 40 input bits, 32 of the bits provide the frequency information, giving an effective frequency resolution of 33 millihertz. The DDS can be programmed in approximately 200 ns and instantaneously jump to any frequency in a 144 MHz band.

IV. Flight Results

The E-Winds sounding rocket campaign was conducted on the night of July 1, 2003 from Wallops Island, Virginia. The mission was a cooperative effort by the University of Texas at Dallas (UTD), Clemson University, the Air Force Research Laboratory (AFRL), and Utah State University (USU) to investigate the spatial and temporal formation of midlatitude plasma layers maintained by neutral winds in the nighttime E-region of the ionosphere. Four rockets were launched at 3:18, 5:41, 6:50, and 7:07 UT, with respective payload numbers of 41.036, 41.037, 27.144, and 41.038. 41.036, 41.037, and 41.038 contained chemical release experiments from Clemson University to optically measure upper atmospheric neutral winds. 27.144 contained an electric field probe, an ion mass spectrometer, and a neutral wind instrument provided by UTD. The USU PIP was present on all four payloads to provide plasma density measurements for the mission. AFRL provided ground-based ionosonde measurements to help determine favorable launch

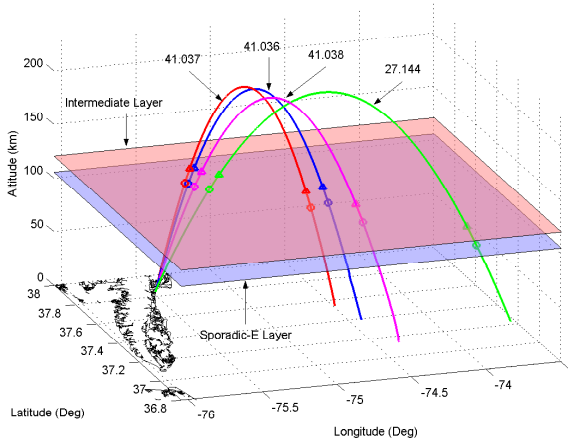

Fig. 3. Sequential Rocket Study of Nighttime Descending Layers (E-Winds) Flight Trajectories

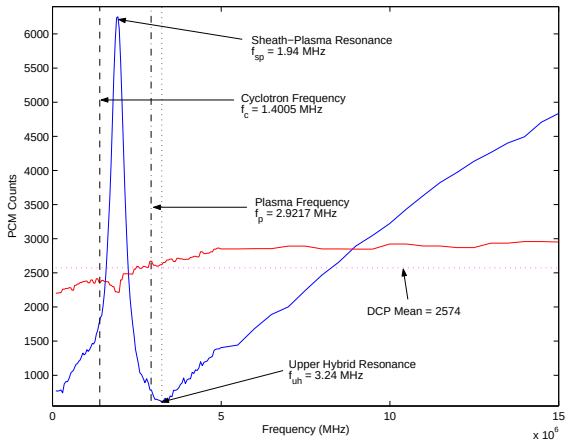

Fig. 4. Analysis of 41.037 PSP and DCP data to obtain α

conditions. The flight trajectory of each payload is shown in Fig. 3.

Fig. 3 shows roughly the existence of two plasma layers that were encountered by each of the rockets, a sporadic-E layer at approximately 102 kilometers and an intermediate layer around 120 kilometers. 41.036, 41.037, and 41.038 attained maximum altitudes of approximately 205 kilometers and 27.144 attained an apogee of 225 kilometers.

With a telemetry rate of 800 kilobits per second, the USU PIP collected over 80 megabytes of raw data for each flight with no telemetry data dropouts. The raw data includes NASA time stamp and header information. Removing the unnecessary NASA data leaves approximately 40 MB of raw science data to analyze for each payload. Data reduction and analysis are being performed in Matlab. Data from the DCP, PFP, PSP, PQP, and IRP has been processed for each of the four payloads and is being analyzed to extract the relevant plasma parameters. The mission was very successful in terms of the operation of the PIP instrument. For the four payloads, only the IRP on 41.036 failed, as the RF head circuitry within the IRP boom was damaged during integration, resulting in a non-functional IRP for 41.036.

A. DCP Data

The DC Langmuir probe data was the first to be analyzed. We may recall that a DCP can provide relative electron densities. The flight DCP data are 14 bit words that must be converted to electron density for analysis. The conversion from counts to electron density may be represented as

$$N_e = \alpha\,(DCP_{counts}) \tag{3}$$

where α is a conversion factor. In order to find α, data from the PSP was used. The factor α can be found by looking at a couple of sweeps near the density peaks that occur near the plasma layers. Near the peak densities, the upper hybrid resonance is easily identified. Using the measured upper hybrid frequency and the cyclotron frequency provided by a magnetic field model, the electron density is computed. By looking at the average of the counts provided by the DCP over the same interval, α is obtained. This procedure is illustrated in figure 4.

Payload 41.037, the second flight of the night was used to compute the α for all the payloads. Figure 4 shows a single frequency sweep for the PSP in blue and the corresponding DCP data given in red. This particular sweep occured at about 104 km on the downleg of the flight. The resonant frequencies for the sweep are computed from the curve characteristics. The upper hybrid resonance corresponds to a minimum in the admittance, occurring at 3.24 MHz. The magnetic field at 104 km above Wallops Island may be computed using the IGRF model, providing a magnetic field strength of 50000 nT, resulting in a electron gyrofrequency of 1.4005 MHz. The plasma frequency can then be computed as the root square difference of f_{uh} and f_c, giving a value of 2.9217 MHz. The corresponding electron density is 1.1871×10^5 cm^{-3} Over the same spatial and temporal interval, the DCP made measurements resulting in the red curve in Fig. 4. Taking the mean of the curve over the interval provides a relatively good measure of the plasma that was seen concurrently by the PSP. The mean for the DCP over the interval was equal to 2574. Substituting the DCP mean and electron density back into (3), we can solve for α giving an α of approximately 50. Using the α that we have computed, the DCP data from the E-Winds campaign was appropriately scaled to give electron density profiles that are shown in Figs. 5-8. It should be noted that α is really a time-varying constant that changes during the

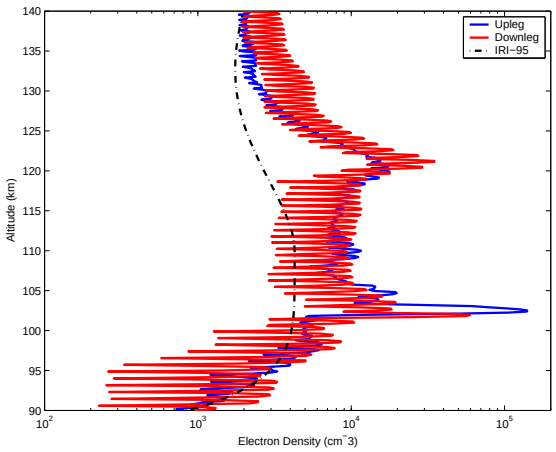

Fig. 5. 41.036 DCP Electron Density Profile (3:19 UT)

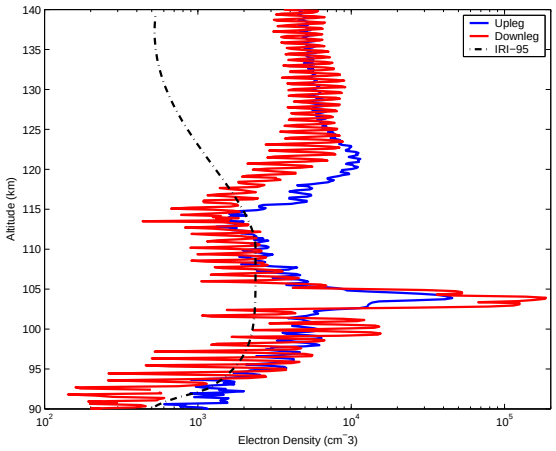

Fig. 6. 41.037 DCP Electron Density Profile (5:41 UT)

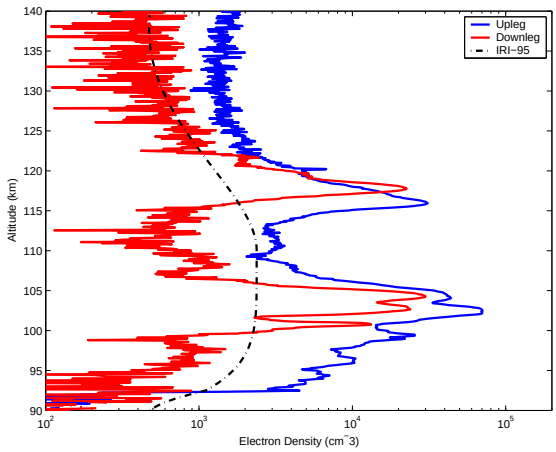

Fig. 7. 27.144 DCP Electron Density Profile (6:50 UT)

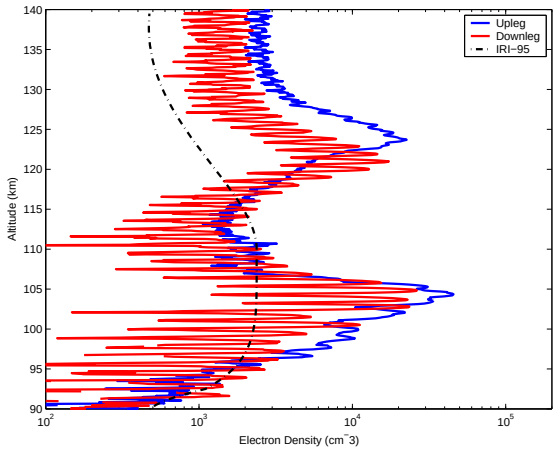

Fig. 8. 41.038 DCP Electron Density Profile (7:07 UT)

course of the flight, but the changes in α should be small, so it is reasonable to assume that it is constant for the entire flight in order to simplify the data analysis.

The electron density profiles in figs. 5-8 clearly show the plasma layers that were encountered by each payload. The blue curves in each plot represent the upleg of the flight and the red curves represent the downleg portion. The black dashed line was produced by the IRI-2001 model for an unperturbed ionosphere over Wallops Island. The altitude range for each of the plots is from 90 to 140 km, which is the region where the plasma layers were located. The first layer, a sporadic-E layer occurred at about 104 km. The second layer, a descending plasma layer existed at about 120 km.

The oscillating noise in each of the figures is due to rocket spin modulation. Payloads 41.036, 41.037 and 41.038 were all spin stabilized at a rate of approximately 2 Hz. As the payload spins through the plasma, a plasma wake where the density is lower is created behind the moving payload. As the DCP boom moves in and out of the wake, the result is a modulating electron density measurement. 27.144 was also spin stabilized, but at a much lower rate of 0.25 Hz, thereby reducing the amount of spin modulation. Some effects of the spin modulation can be reduced by downsampling the DCP data.

B. PFP Data

With the DCP data providing a basis for the location of the layers and relative electron density, the data for the impedance instruments, the PFP, PSP, and PQP can be comparatively analyzed. The PFP was somewhat experimental for this flight due to a new digital control system for the instrument. Additionally, the PFP technique is often not successful in the nighttime E-region of the ionosphere due to the collisional damping of the plasma resonances.

The PFP was unable to lock onto the upper hybrid resonance for the 41.036, 41.037, and 27.144 payloads. For 41.036 and 41.037, the inability of the PFP to lock was due to two principal problems. First, the plasma density during the ma-

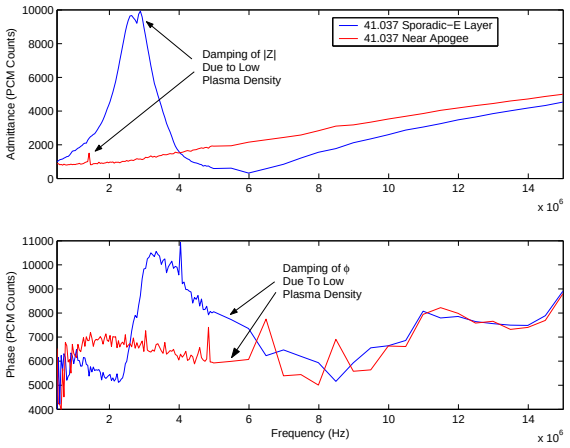

Fig. 9. Damping of Admittance and Phase for Flight 41.037

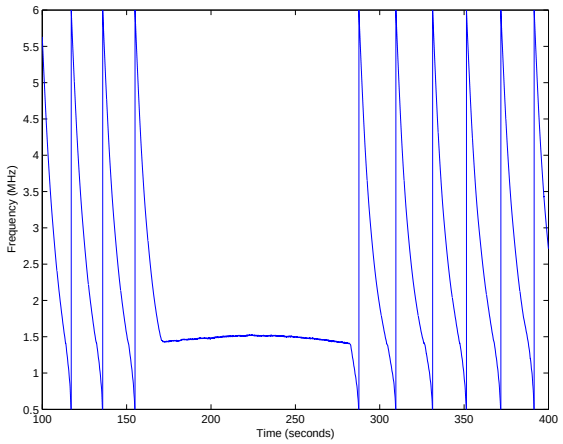

Fig. 10. 41.038 PFP Lock Frequency Versus Time

jority of the flight was too low. Second, the PFP control gain was too low to effectively acquire and maintain phase lock on the noisy phase signal.

Below 130 km the instrument displayed significant damping in the magnitude and phase responses. The damping was a result of the large free space impedance of the monopole antenna and collisional damping within the plasma between the electrons and neutral particles. In this dilute, collisional plasma the number of oscillating electrons at the resonant plasma frequencies was not sufficient to effective couple energy back onto the antenna, resulting in a damped frequency response. To illustrate the effect of the damping for the second flight, 41.037, the magnitude and phase curves from the PSP instrument have been plotted in Fig. 9. The blue curve in the figure corresponds to a PSP measurement in the sporadic-E layer, while the red curve corresponds to a measurement in a dilute plasma somewhere near apogee. In the sporadic-E layer, the electron density increases by nearly two orders of magnitude leading to efficient energy coupling at the sheath-plasma and upper hybrid resonances enhancing the curves at the resonances. When the density is below about $10^3 cm{-}3$, the plasma cannot sufficiently influence the free space impedance of the monopole, resulting in poor phase measurements that look strictly capacitive. Hence the PFP is capable of measuring densities above 1000 electrons per cubic centimeter.

The other reason that the PFP had difficulty in acquiring and maintaining lock is due to the loop control gain of 1. This small control gain did not allow the PFP to search through the frequency band of interest fast enough in its lock acquisition mode. When coupled with the poor phase response due to low plasma density, the PFP could not acquire and maintain phase lock for 41.036 and 41.037.

The PFP aboard 27.144 also did not function. However, in preliminary data reduction and analysis, it appears that the either the instrument was damaged during integration and test or was interfered with by a naval radar that could have been tracking the payload.

Fortunately, the PFP locked for a significant portion of 41.038 near the trajectory's apogee as shown in Fig. 10. The flight occurred late enough into the night that the bottom of the F-region had descended near the apogee of the payloads enriching the region with plasma. The instrument was locked for over 100 seconds of the 400 second flight at frequencies near 1.5 MHz. Fig. 10 demonstrates the slow lock acquistion time of the E-Winds PFP in the plasma. Due to the unity control gain, the lock acquisition time in the plasma environment averaged about 23 seconds for a sweep from 6 MHz down to the reset frequency of 500 kHz.

When locked, the PFP provided a high temporal resolution measurement of the upper hybrid frequency. The PFP locked on the upleg of the flight near 188 kilometers and lost lock on the downleg near 188 kilometers, so the instrument was locked over a distance of approximately 40 kilometers near apogee.

Assuming a constant cyclotron frequency, f_c, for the small altitude range, the electron density can be computed according to (1). For a quantitative comparison, the resulting electron density from the PFP can be compared against the DCP data over the same altitude range. Fig. 11 shows the upleg portion of the flight and Fig. 12 shows the downleg of the flight.

On the upleg, the two measurements agreed fairly well, but the PFP measures small-scale variations in the plasma that the DCP is not able to respond to. This could be due to a capacitive effect on the DCP because of contamination. On the downleg, the PFP and DCP measurements are

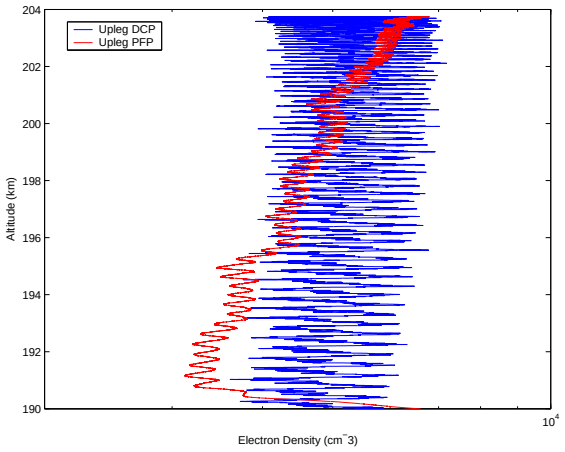

Fig. 11. 41.038 Upleg PFP Electron Density Vs. DCP Electron Density

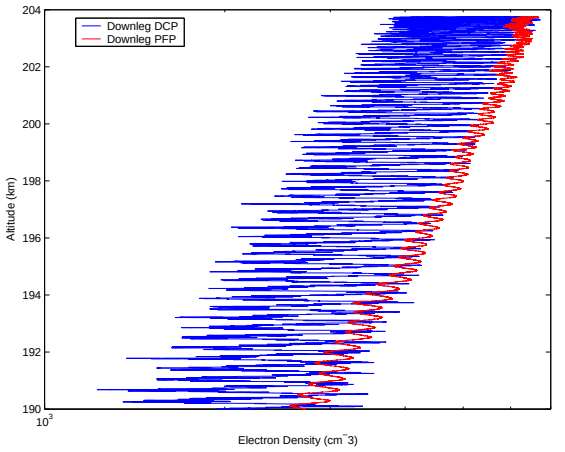

Fig. 12. 41.038 Downleg PFP Electron Density Vs. DCP Electron Density

very close to one another. The closeness of the measurements on the downleg gives a measure of confidence in the DCP data.

The DCP and PFP were mounted in a transverse configuration, so that the booms were 180^o out of phase with one another. This can clearly be seen in both the figures. A maximum in the PFP measurement corresponds to a minimum in the DCP measurement and vice versa.

C. PSP, Q, and IRP Data

The data from the last three instruments of the PIP, the PSP, PQP, and IRP have not been extensively analyzed due to calibration issues and time constraints. Due to a small amount of coupling between the magnitude and phase channels and the nonlinearity of the log amp used for magnitude detection, a mathematical calibration model of the instrument has been difficult to determine. This calibration is needed to appropriately scale the PSP, Q, and IRP data from PCM counts to impedance in Ohms. This calibration issue is under considerable scrutiny at the present time.

The PSP data has already provided a wealth of knowledge about the resonant frequencies in the plasma. Thus far, the PSP data has been used to compute the α for the correct scaling of the DCP data. The PSP data was also used to validate the nonlocking behavior of the PFP. Once a calibration is performed, curve fitting to the PSP data will provide absolute electron density measurements for each flight.

The PQP measurements are made around the lock frequency, implying that the experimental Q data for the campaign will be determined from the 100 seconds of data acquired during when the PFP was locked for 41.038. A full analysis of the Q data will also depend on the post-flight calibration of the instrument. Impedances in Ohms are needed to fully characterize the Q of the upper hybrid resonance.

The experimental IRP provided an interesting set of data on the downleg of 41.037 within the sporadic-E layer. The downleg sporadic-E layer on 41.037 was the densest layer encountered during any of the flights. At the peak density of the layer around 102 km, a distinct resonance occurred near 24 kHz. More analysis is needed to understand exactly what the resonance represents, but the resonance could correspond to the lower hybrid frequency. If the instrument really measured the lower hybrid resonance, then the IRP is the first impedance instrument to successfully probe the ionosphere for the lower hybrid frequency. Because the effect occurred only once during a single sweep, additional flights of the IRP into a dense plasma, like the daytime F-region, are needed to determine whether the instrument is capable of measuring the lower hybrid resonance.

V. Conclusion

The PIP instrument that flew as part of NASA's E-Winds sounding rocket campaign proved to be a success for a number of reasons. First and foremost, the PIP was designed, built, tested, and calibrated primarily by students at USU. Such an opportunity provided invaluable experience for the students involved in designing and testing real space instrumentation. Second, the new RF head design for the instrument was stable and extremely sensitive to small changes in the plasma environment. Third, the digital control system for the PFP proved successful in challenging plasma conditions. Fourth, the multiple measurements made by each of the PIP instruments provided a fully redundant data set for determining electron density. Finally, the experimental IRP demonstrated that it may be useful in determining resonances that have not been previously measured in the ionosphere using impedance methods.

A further refined PIP instrument will gain additional flight experience in the summer of 2004 on board the Kwajalein-Hysell sounding rocket campaign. Data from this future mission will further validate the new PIP and its usefulness in determining plasma parameters in the ionosphere.

References

[1] R.D. Leach and M.B. Alexander "Failures and Anomalies Attributed to Spacecraft Charging." *NASA/RP-1375*, NASA Marshall Space Flight Center, 1995.

[2] T. Bandyopadhayay, et. al. "Degradation of navigational accuracy with global positioning system during periods of scintillation at equatorial latitudes." *Electronics Letters*, vol. 33, no. 12, pp. 1010-1011, Jun. 1997.

[3] J.M Goodman and J. Aarons "Ionospheric effects on modern electronic systems." *Proceedings of the IEEE*, vol. 78, no. 3, pp. 512-528, Mar. 1990.

[4] G. Blais and P. Metsa "Operating the Hydro-Quebec grid under magnetic storm conditions since the storm of March 13, 1989." *Proc. Solar-Terrestrial Predictions Workshop, Ottawa, May 18-22, 1992*, pp. 108-130, 1993.

[5] L.H. Brace "Langmuir Probe Measurements in the Ionosphere." *Measurement Techniques in Space Plasmas: Particles*, American Geophysical Union, 1998.

[6] J.E. Jackson and J.A. Kane, "Measurement of ionospheric electron density using an RF probe technique." *J. Geophys. Res.*, vol. 64, pp. 1074-1075, Aug. 1959.

[7] K.D. Baker and M.D. Jensen, "Measuring ionospheric electron density using the plasma frequency probe." *J.Space.Rockets*, vol. 29, pp. 91-95, Jan.-Feb. 1992.

[8] E.J. Lund, et. al., "The Plasma Frequency Tracker: An Instrument for Probing the Frequency Structure of Narrow-Band MF/HF Electric Fields." *Measurement Techniques in Space Plasmas: Fields*, American Geophysical Union, 1998.

[9] K.G. Balmain, "The impedance of a short dipole antenna in a magnetoplasma" *IEEE Trans. Antennas and Propagation*, vol. AP-12, pp. 605-617, September 1964